

Temperature dependence of damage accumulation in α -zirconium

C. Arévalo ^{a,*}, M.J. Caturla ^b, J.M. Perlado ^a

^a *Instituto de Fusión Nuclear, Universidad Politécnica de Madrid, Spain*

^b *Universidad de Alicante, Dep. Física Aplicada, Alicante, Spain*

Abstract

Using the input data obtained from molecular dynamics (MD) simulations on defect energetics and cascade damage, we present results obtained on irradiation of hexagonal-close-packed (hcp) α -zirconium under different conditions with a kinetic Monte Carlo (kMC) model. We used three 25 keV cascade databases at temperatures of 100 K, 300 K and 600 K respectively. The evolution of the microstructure during irradiation for a dose rate of 10^{-6} dpa/s, at temperatures of 100 K, 300 K and 600 K until a final dose of 0.1 dpa has been studied. We have considered isotropic motion for vacancies and one dimensional movement for interstitials and we have studied how the accumulation of damage is affected considering different temperatures. We present preliminary comparisons with experimental data.

© 2007 Published by Elsevier B.V.

1. Introduction

Radiation damage in hexagonal-close-packed (hcp) metals is different from that of the face-centered cubic (fcc) or body-centered (bcc) metals [1,2]. In contrast with fcc and bcc cases, radiation damage in hcp metals varies from one hcp metal to another. In particular, in the case of Zr, vacancy and self-interstitial type of loops are observed under TEM both in electron and neutron irradiation [3]. Moreover, the relative proportion of vacancy to self-interstitial dislocation loops depends strongly on temperature. Interpretation of these experimental observations requires of detail knowledge of

the atomistic processes occurring during irradiation in hcp metals, including defect formation, migration and growth.

Molecular dynamics (MD) is a powerful tool to obtain atomic-scale information and it can provide data about the initial damage during the collisional cascade. However, the time scales addressed by this method are only up to a few nanoseconds. In order to understand the evolution of the accumulated damage for long times at a microscopic scale, it is necessary to use other simulation techniques such as rate theory or kinetic Monte Carlo (kMC).

In this paper we present a study of the evolution of the microscopic damage in hcp Zr under continuum irradiation, and the dependence on temperature, with a kMC approach using cascade data from MD simulations. We present the evolution of defect concentration (vacancies and interstitials)

* Corresponding author. Tel.: +34 913363108; fax: +34 913363002.

E-mail address: cristina@denim.upm.es (C. Arévalo).

versus dose for three different temperatures (100 K, 300 K and 600 K), the cluster size distribution, that is, the number of defects as a function of the size for a dose of 0.01 dpa and 0.1 dpa, and the maximum size for vacancies and interstitial versus temperature for these two different doses. The results obtained are contrasted with the experimental data available and some conclusions are drawn regarding the migration mechanisms and assumptions of the model.

2. Temperature dependence of damage accumulation in hcp metals

Using MD, a database of displacement cascades for hcp α -zirconium was generated by Bacon et al. [4]. As input for our simulations, we have used cascades produced by recoils of 25 keV at 100 K, 300 K and 600 K. Information about migration, binding energies, and pre-factors of the different cluster sizes and types have also been obtained using MD and they have been introduced in our simulations. Molecular dynamics simulations of formation energies of interstitial clusters show high stability of these clusters, with binding energies on the order of 2 eV. Jump frequencies for self-interstitials were taken from the function [5,6]

$$v_n = v_0 n^{-S} \exp(-\langle E_m \rangle / k_B T), \quad (1)$$

where $\langle E_m \rangle$ is a general migration energy (0.015 eV), $S = 0.56$ and $v_0 = 2.6 \times 10^{12} \text{ s}^{-1}$. Binding energies for a vacancy to a cluster of n vacancies have been obtained from the formula [7]

$$E_b^V(n) = 1.74 - 2.61(n^{2/3} - (n-1)^{2/3}) \text{ eV}. \quad (2)$$

The migration energy for single vacancies is 0.93 eV [5] with an attempt frequency of $1.22 \times 10^{14} \text{ s}^{-1}$. Further details of the parameters used are given in Refs. [5–8]. The kinetic Monte Carlo code called BIGMAC was used and modified for these calculations [9].

In order to understand damage accumulation in hcp metals and study the dependence on temperature, we introduced the MD cascades [4] as initial damage and we studied the evolution of the microstructure (defect cluster diffusion) for long times (hours). The size of the computational box was $100 \times 100 \times 100 \text{ nm}^3$. A dose rate 10^{-6} dpa/s until a final dose of 0.1 dpa and periodic boundary conditions were used. We carried out three types of calculations depending on the temperature: 100 K, 300 K and 600 K. For each of these simulations, the corre-

sponding 100 K, 300 K and 600 K 25 keV cascade database were placed in a random way in the box and were repeated in the system in order to simulate the damage accumulation until the final dose was reached. We have considered one dimensional (1D) motion for Single Interstitial Atoms (SIAs) and mobile interstitial clusters and 3D motion for monovacancies. Interstitial clusters have been identified from the MD simulations; there are mobile and immobile ones and such a characteristic is carried into the kMC model. The mobile interstitial clusters are loops with Burgers vector $1/3\langle 11-20 \rangle$, while the immobile ones are three-dimensional irregular clusters. Vacancy clusters are supposed to be immobile. Due to the fast migration energy of SIA and SIA clusters and their low 1D migration, we have introduced a grain boundary approximation: grain size of $1 \mu\text{m}$. That means that if one defect moves more than $1 \mu\text{m}$ without finding another one, it disappears in a sink.

Since most of the experimental data available, to the best of our knowledge, consists of TEM studies we have analyzed the results of our calculations in terms of visible clusters under TEM. We consider visible those clusters that include more than 50 defects, which correspond to loops of about 2 nm in radius.

Fig. 1 shows visible vacancy clusters concentration for three different temperatures versus dose until a final dose of 0.1 dpa. The highest concentration for any given dose is at 600 K, and the lowest concentration occurs at 100 K; we have also observed that, at 600 K, visible clusters appear at earlier doses.

The opposite behavior takes place with visible interstitials clusters as presented in Fig. 2. At 600 K we almost have found no visible interstitials and at 100 K and 300 K interstitials appear in the same concentration and at the same dose.

Fig. 3 shows the vacancy cluster size distribution (that is the number of clusters versus cluster size in the form of number of defects in a cluster) at the same three temperatures for two doses: 0.01 dpa and 0.1 dpa. We have represented group sizes (not all the sizes) starting by five (sum of clusters that have from two to five defects), then ten (the sum of clusters from six to ten) and then in steps of ten. At 100 K and 300 K, size distribution goes from the smallest sizes (higher number of clusters) to the largest ones (lower values). At 600 K, the curve has a different shape; there are not small clusters, because small vacancy clusters dissolve at this temperature and migrate effectively, as joining those

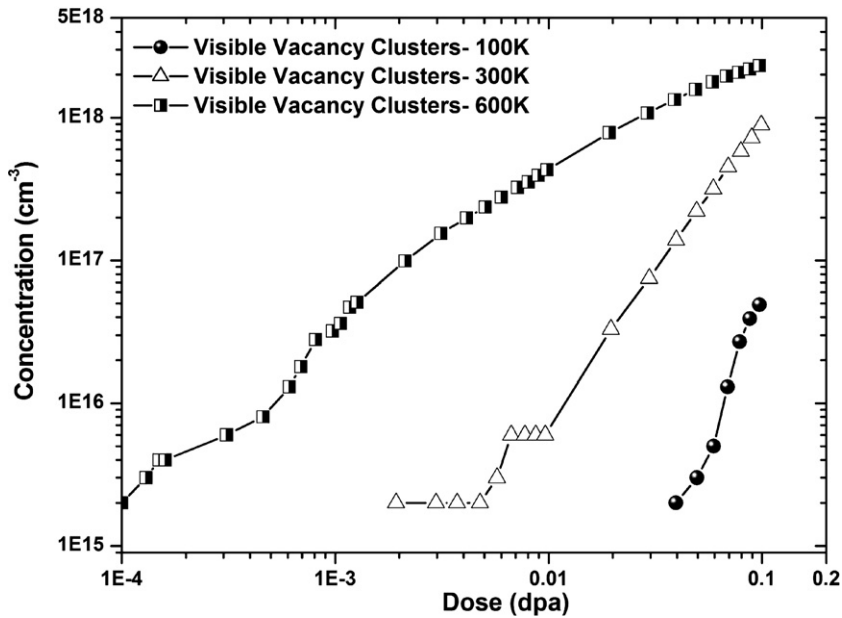


Fig. 1. Visible vacancy concentration versus dose at 100 K, 300 K and 600 K.

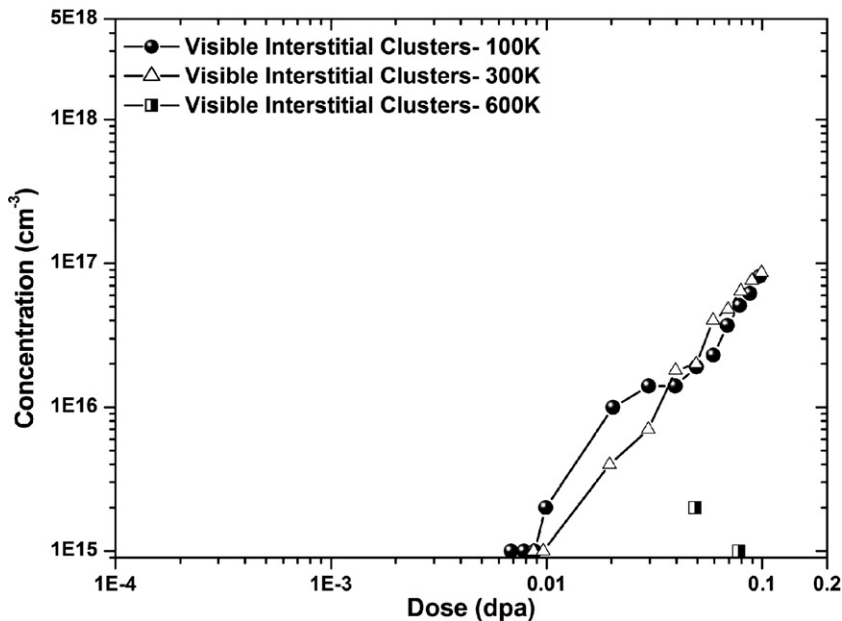


Fig. 2. Visible interstitial concentration versus dose at 100 K, 300 K and 600 K.

of largest size. It can be also noticed that whereas, at 100 K and 300 K the dose increases and curves move towards higher concentration with no changes in size distribution clusters, at 600 K there is not much of an increase in the number of clusters but rather in the size of the clusters.

In the case of interstitial size distribution, as is shown in Fig. 4, the curve shape at the three temperatures is similar and similar to that for vacancies at 100 K and 300 K (size distribution with higher number of clusters in smaller size and lower number of clusters at higher sizes). When the temperature

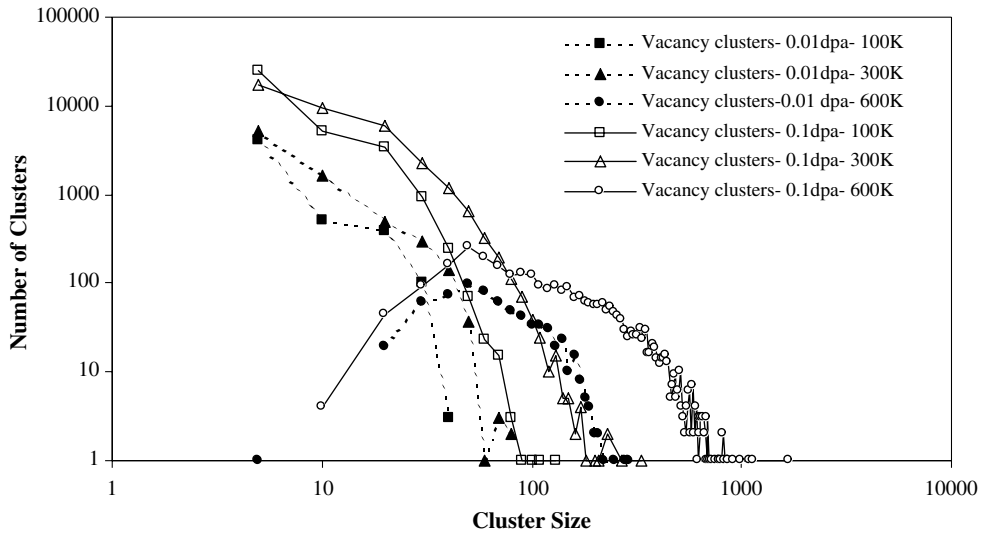


Fig. 3. Vacancy cluster size distribution at 100 K, 300 K and 600 K for doses of 0.01 dpa and 0.1 dpa.

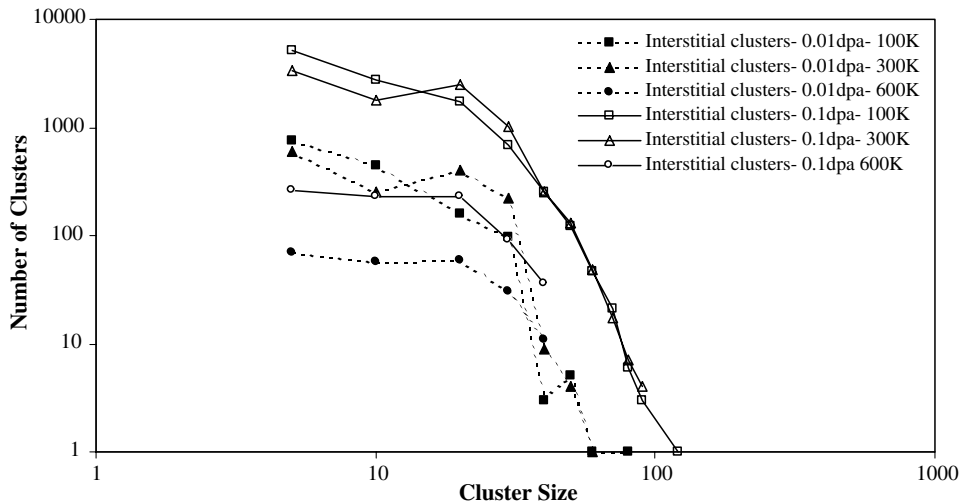


Fig. 4. Interstitial cluster size distribution at 100 K, 300 K and 600 K for a doses of 0.01 dpa and 0.1 dpa.

increases, higher interstitial clusters disappear, which it is an opposite result in comparison with vacancies. At 100 K and 300 K, the size of interstitial clusters increases with dose, but at 600 K, it remains constant.

3. Discussion

Fig. 5 shows the concentration of visible vacancy clusters as a function of temperature for a dose of 0.1 dpa (left y-axis). This increase in concentration of visible vacancy clusters with temperature can be explained by the mobility of vacancies together with

the binding energy of small vacancy clusters. At 600 K, vacancies are mobile but small vacancy clusters are unstable. Ostwald ripening then occurs at this temperature as Fig. 3 shows; for this temperature, the concentration of small vacancy clusters is low and the distribution shifts towards larger cluster sizes. In Fig. 5, we also represent the concentration of visible interstitial clusters (right y-axis). In this case the concentration of visible interstitial clusters is very similar for 100 K and 300 K, while no interstitial clusters larger than 50 are observed at 600 K. In this case, the mobility of single vacancies and release of vacancies from small clusters results in

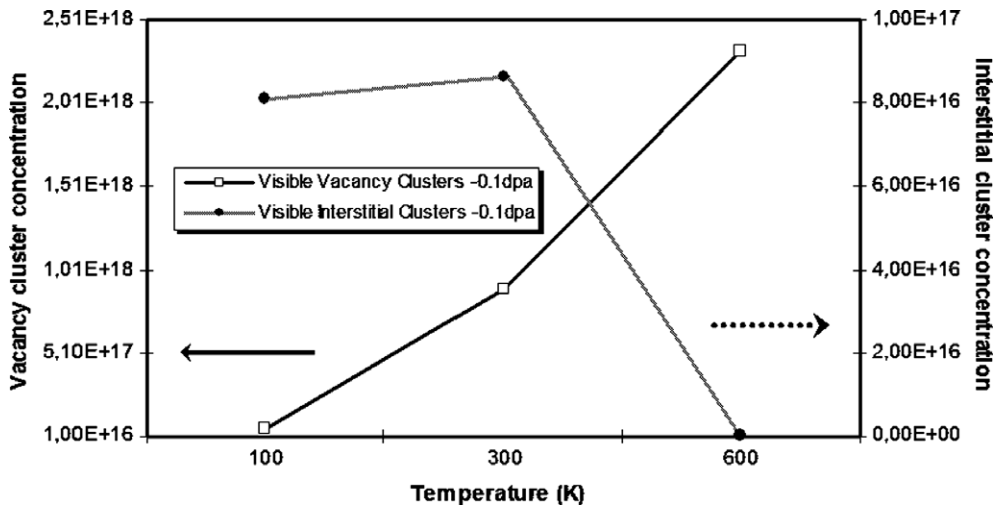


Fig. 5. Visible concentration (per cubic centimeter) for vacancies and interstitials versus temperature for a dose of 0.1 dpa.

enhanced recombination between vacancies and immobile interstitial clusters, and therefore a decrease in interstitial cluster concentration. Notice that in Fig. 4 the change in temperature only results in a reduction of concentration for all interstitial cluster sizes, a very different behavior from that observed for vacancies in Fig. 3. Fig. 5 also shows that at low temperature (100 K) the concentration of visible interstitial clusters is higher than that of visible vacancies ($8 \times 10^{16} \text{ cm}^{-3}$ versus $4.9 \times 10^{16} \text{ cm}^{-3}$). The transition temperature is 300 K with visible vacancy concentration higher than the interstitial concentration, while, at 600 K, only vacancy clusters are observed.

Fig. 6 shows the maximum vacancy and self-interstitial cluster sizes as a function of temperature (left and right y-axis respectively). Like in the case

of concentration, the vacancy clusters increase in size with temperature while the size of the interstitials decrease. Notice that this behavior is not linear with temperature, clearly seen for the vacancy clusters. The increase at 300 K is due to single vacancy migration as well as larger cluster sizes from the MD simulations. For 600 K, dissolution of small vacancy clusters enhances the growth towards even larger cluster sizes. This is also reflected in the reduction of interstitial cluster size, which is again not linear with temperature.

As reported by Griffiths [10], neutron irradiation experiments of Zr at low temperature (lower than 350 K) show vacancy cluster concentrations lower than the interstitial concentration, while at temperatures between 573 K and 723 K the concentration of vacancies is higher than that of interstitials. More

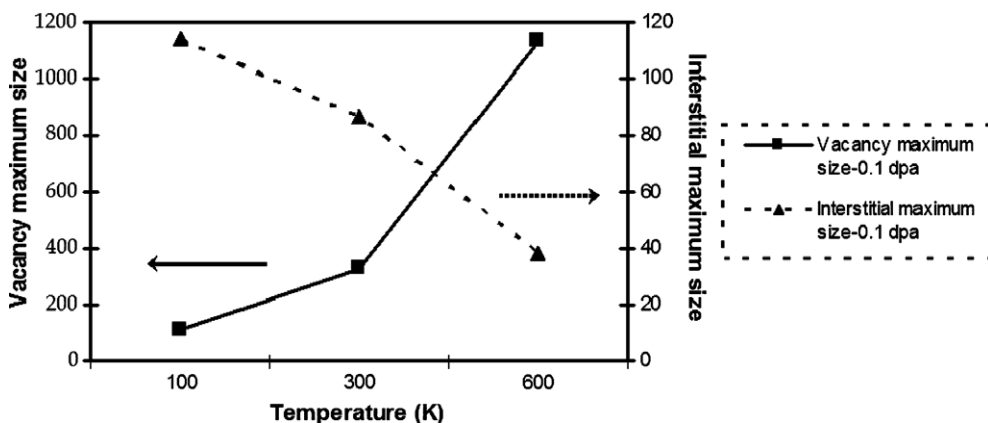


Fig. 6. Maximum size for vacancies and interstitials versus temperature for a dose of 0.1 dpa. The size is given in number of defects.

specifically, Griffiths [10] reports that under neutron irradiation at about 573 K there is approximately equal number of vacancies (52%) than interstitials (48%) loops, while at 673 K 70% of the defects are vacancy type. Although our calculations were not aimed towards a direct comparison with these experimental measurements, they are in qualitative good agreement both for the relative changes in concentration and the temperature at which the transition occurs, and provide an explanation for this behavior.

Some significant differences between the experimental observations and the results of our simulations must be noted. On one hand, defect concentrations are always higher than those observed experimentally, at least for vacancy type of defects. In particular, Hashimoto et al. [11] reports concentrations of defects under neutron irradiated Zr of $6.5 \times 10^{16} \text{ cm}^{-3}$ for a dose of 0.63 dpa and a temperature of 353 K. On the other hand self-interstitial cluster sizes are always much smaller than vacancy clusters from these simulations, which contradicts some of the experimental observations [10].

Two factors in the model could explain these differences. One dimensional migration was assumed for the motion of self-interstitial clusters of all sizes and for all temperatures, which results in the removal of practically all of the mobile interstitial clusters at grain boundaries without any interaction with vacancies or immobile interstitials. For the highest temperature studied here, 600 K, it is possible that a two dimensional mechanism of migration operates. This will result in higher recombination, reducing the vacancy cluster size and increasing the interstitial sizes. These calculations are currently being performed. The presence of impurities could also affect the one dimensional migration of these clusters. The second effect is that the large vacancy cluster sizes observed at the lower temperatures are related to the initial cluster sizes obtained from MD simulations.

Finally, we should point out that in order to make a real comparison between experiments and simulations, the visible cluster size from TEM experiments must be resolved. This could be done with the help of TEM image simulations from MD calculations of loops of different sizes and types.

4. Conclusions

We have performed kMC calculations of damage accumulation in α -Zr under continuum irradiation at 100 K, 300 K and 600 K using input parameters from MD simulations. These calculations show an increase in vacancy cluster concentration with temperature and a decrease in interstitial concentration. This is due to the mobility of single vacancies and the instability of small vacancy clusters at 600 K, resulting in recombination of vacancies with immobile interstitials at this temperature and vacancy cluster growth. These results are in qualitative good agreement with experimental observations of irradiated α -Zr. However, further improvements must be done to the model in order to have quantitative comparison with experimental results.

Acknowledgements

We want to thank N. de Diego for references and R. Voskoboinikov and D.J. Bacon for MD cascades; to all of them for very useful discussion. This work has been performed under funding of EURATOM-project FIKS-CT-2001-00137 (SIRENA) title 'Simulation of radiation effects in Zr–Nb alloys: Application to stress corrosion cracking behavior in iodine-rich environment'. One of the authors (MJC) wants to thank the Ministerio de Educación y Ciencia in Spain for support under the Ramon y Cajal program.

References

- [1] D.J. Bacon, F. Gao, Y.N. Osetsky, J. Nucl. Mater. 276 (2000) 1.
- [2] M. Kiritani, J. Nucl. Mater. 276 (2000) 41.
- [3] M. Griffiths, J. Nucl. Mater. 205 (1993) 225.
- [4] R.E. Voskoboinikov, Yu.N. Osetsky, D.J. Bacon, Nucl. Instrum. and Meth. B, in press.
- [5] Y.N. Osetsky, D.J. Bacon, N. de Diego, Metall. Mater. Trans. A 33 (2002) 777.
- [6] N. de Diego, Y.N. Osetsky, D.J. Bacon, Metall. Mater. Trans. A 33 (2002) 783.
- [7] D. Kulikov, L. Malerba, M. Hou, Nucl. Instrum. and Meth. B 228 (2005) 245.
- [8] C. Arévalo, M.J. Caturla, J.M. Perlado, Proc. MRS 792 (2003) 642.
- [9] M.D. Johnson, M.J. Caturla, T. Diaz de la Rubia, J. Appl. Phys. 84 (1998) 1963.
- [10] M. Griffiths, J. Nucl. Mater. 159 (1988) 190.
- [11] N. Hashimoto, T.S. Byun, K. Farrell, S.J. Zinkle, J. Nucl. Mater. 947 (2004) 329.